OPEN ACCESS
CellPress

Cell Reports
Resource

Fly-FUCCI: A Versatile Tool for Studying Cell Proliferation in Complex Tissues

Norman Zielke,[1] Jerome Korzelius,[1] Monique van Straaten,[1] Katharina Bender,[1] Gregor F.P. Schuhknecht,[1] Devanjali Dutta,[1] Jinyi Xiang,[1] and Bruce A. Edgar[1,*]
[1]Deutsches Krebsforschungszentrum (DKFZ), Zentrum für Molekulare Biologie der Universität Heidelberg (ZMBH) Allianz, Im Neuenheimer Feld 282, 69120 Heidelberg, Germany
*Correspondence: b.edgar@dkfz-heidelberg.de
http://dx.doi.org/10.1016/j.celrep.2014.03.020

SUMMARY

One promising approach for in vivo studies of cell proliferation is the FUCCI system (*f*luorescent *u*biquitination-based *c*ell *c*ycle *i*ndicator). Here, we report the development of a *Drosophila*-specific FUCCI system (Fly-FUCCI) that allows one to distinguish G1, S, and G2 phases of interphase. Fly-FUCCI relies on fluorochrome-tagged degrons from the Cyclin B and E2F1 proteins, which are degraded by the ubiquitin E3-ligases APC/C and $CRL4^{Cdt2}$, during mitosis or the onset of S phase, respectively. These probes can track cell-cycle patterns in cultured *Drosophila* cells, eye and wing imaginal discs, salivary glands, the adult midgut, and probably other tissues. To support a broad range of experimental applications, we have generated a toolkit of transgenic *Drosophila* lines that express the Fly-FUCCI probes under control of the UASt, UASp, QUAS, and *ubiquitin* promoters. The Fly-FUCCI system should be a valuable tool for visualizing cell-cycle activity during development, tissue homeostasis, and neoplastic growth.

INTRODUCTION

The last decades have yielded a detailed understanding of the regulatory networks that govern the eukaryotic cell cycle (Nasmyth, 2001). Most of these groundbreaking studies were conducted in unicellular organisms, early embryos, and immortalized cells grown in culture. Studies of animal cell cycles in their normal context, in cells embedded in complex tissues and regulated by a host of intrinsic and extrinsic signals, have lagged behind. The standard methods used for cell-cycle analysis have all been fixed time point ("snapshot") techniques: labeling of fixed cells (e.g., with bromodeoxyuridine), flow cytometry, and lineage tracing. In 2008, Sakaue-Sawano et al. (2008) revolutionized cell-cycle analysis in living cells with their introduction of a novel method that allows the monitoring of cell-cycle phase transitions in living cells, named FUCCI (*f*luorescent *u*biquitination-based *c*ell *c*ycle *i*ndicator). This system, first generated for mice and mammalian cells, relies on two ubiquitin ligases, APC/C and SCF^{Skp2}, whose activities are temporally separated during cell-cycle progression (Sakaue-Sawano et al., 2008; Vodermaier, 2004). The APC/C is active from midmitosis through G1, whereas SCF^{Skp2} is active in S and G2 phases. In the original FUCCI system the activity of these ubiquitin ligases was visualized with green or red-fluorescent proteins fused to degron-containing but otherwise inert fragments of the APC/C substrate, Geminin (aa 1–110), or the SCF^{Skp2} substrate, Cdt1 (aa 30–120) (Sakaue-Sawano et al., 2008). The N terminus of Geminin contains a Destruction (D)-box degron that is sufficient to confer APC/C-mediated degradation, but not the domain required for Geminin's cellular function as an inhibitor of Cdt1 (McGarry and Kirschner, 1998). The Cdt1 degron includes the Cy motif, which endows substrate recognition by the SCF^{Skp2} E3 ligase (Nishitani et al., 2006). The combined expression of both FUCCI probes marked cells residing in G1 phase by red fluorescence, whereas cells in S, G2, and M phases were labeled green. This FUCCI system proved to be a versatile tool for the analysis of various aspects of cell proliferation, including the characterization of cell-cycle oscillations (Santos et al., 2012; Spencer et al., 2013), the response to DNA damage (Davoli and de Lange, 2012; Davoli et al., 2010; Kleiblova et al., 2013), the impact of growth (Son et al., 2012), the coordination with developmental processes (Ogura et al., 2011), the screening for compounds modulating proliferation (Choi et al., 2013; Sakaue-Sawano et al., 2011), and the analysis of differentiation in stem cell lineages (Calder et al., 2013; Coronado et al., 2013; Pauklin and Vallier, 2013; Roccio et al., 2013).

SCF^{Skp2} recognizes the Cdt1-based FUCCI probe via the Cy motif (Nishitani et al., 2006), which is only found in mammals. However, degradation of full-length, native Cdt1 is also mediated by the S phase-specific E3-ligase $CRL4^{Cdt2}$, which recognizes a N-terminal PIP box (Arias and Walter, 2006; Nishitani et al., 2006). The replacement of the Cy motif-based G1 sensor by a PIP box-containing fragment of Cdt1 eventually allowed the development of functional FUCCI systems for zebrafish (Sugiyama et al., 2009) and the urchordate *Ciona intestinalis* (Ogura et al., 2011). However, the G1 sensor based on hCdt1 (aa 30–120) failed to work properly in flies (A. Teleman, personal communication).

Here, we report the development of a functional FUCCI system for *Drosophila* based on degrons from E2F1 and CycB. This design allows assigning different combinations of fluorochromes to cells residing in G1, S, or G2 phase, thus allowing the accurate

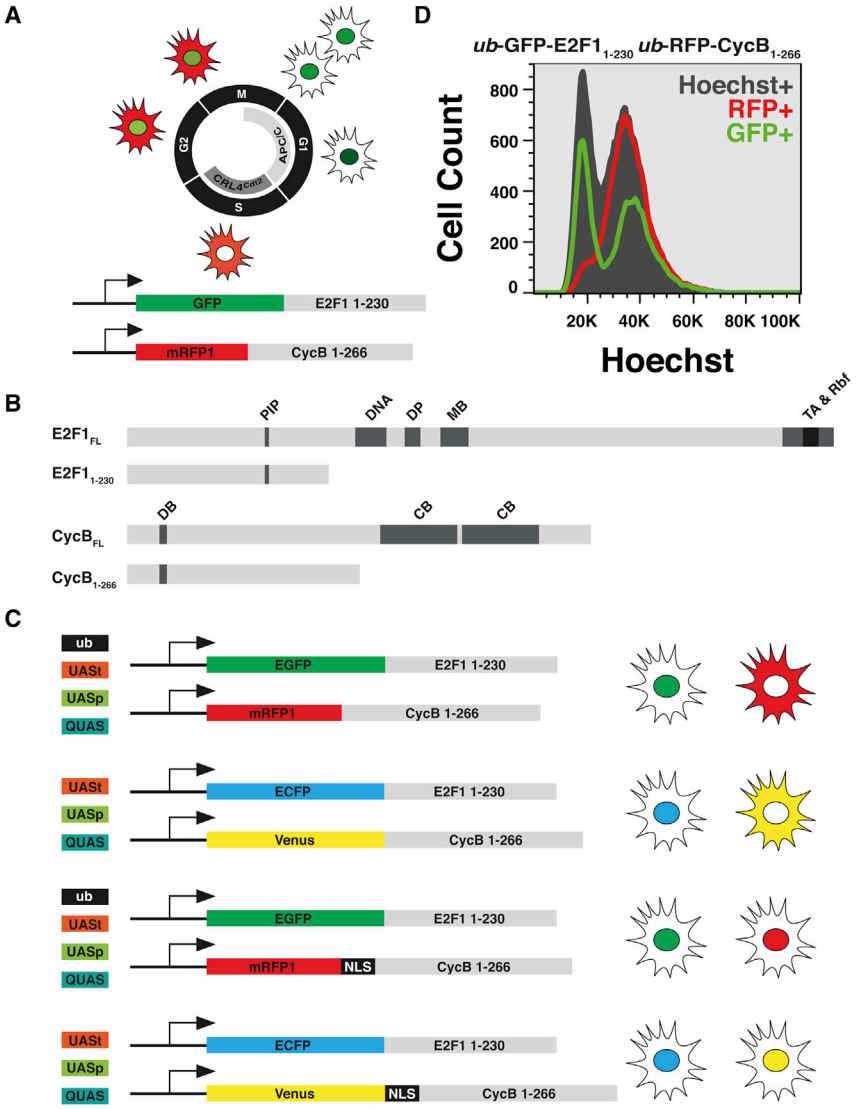

Figure 1. The Fly-FUCCI System: A Toolkit for the In Vivo Analysis of Cell-Cycle Phasing

(A) Concept of the Fly-FUCCI system. In early M phase, both GFP-E2F1$_{1–230}$ and mRFP1-CycB$_{1–266}$ are present thus labeling the cells yellow. In mid-mitosis, the APC/C marks mRFP1-CycB$_{1–266}$ for proteasomal degradation leaving the cells fluorescing green due to GFP-E2F1$_{1–230}$ expression. As cells progress from G1 to S phase, CRL4^{Cdt2} degrades GFP-E2F1$_{1–230}$, and cells are thus labeled in red, because only mRFP1-CycB$_{1–266}$ is present. After cells enter G2 phase, GFP-E2F1$_{1–230}$ protein levels reaccumulate, marking the cells yellow due to the presence of mRFP1-CycB$_{1–266}$.

(B) Schematic of the utilized fragments of E2F1 and CycB. Full-length E2F1 protein (E2F1$_{FL}$) contains a PCNA-interaction protein (PIP) box; a DNA-binding domain (DNA); a Dp-dimerization domain (DP); a marked box (MB); as well as a transactivation and Rbf1 binding domain (TA & RBF). Full-length CycB protein (CycB$_{FL}$) includes a destruction box (DB) and two Cyclin box (CB) domains. The fragments used for constructing the Fly-FUCCI system, E2F1$_{1–230}$ and CycB$_{1–266}$ only include the PIP and DB degrons.

(C) The collection of Fly-FUCCI strains includes multiple variants that can be expressed under control of the indicated promotors (*ub*, UASt, UASp, and QUAS). For convenience, GFP/CFP-E2F1$_{1–230}$ and mRFP1/Venus-CycB$_{1–266}$ or mRFP1/Venus-NLS-CycB$_{1–266}$ were recombined either on the second or third chromosome.

(D) FACS profile of dissociated wing disc cells expressing *ub*-GFP-E2F1$_{1–230}$ and *ub*-mRFP1-CycB$_{1–266}$. GFP-positive cells were mostly found in the G1 and G2 peak, whereas RFP expression correlated with S and G2 phase. Black profile depicts DNA.

tracking of cell-cycle phase transitions. Moreover, the original FUCCI sensors were ubiquitously expressed in all cells, making it difficult to identify and track specific cell populations in tissues of more than one cell layer, or in complex organs. We solved this problem by using the Gal4/UAS and QF/QUAS bipartite transcription control systems, which allow the FUCCI probes to be targeted to nearly any desired cell type in the fly. Here, we describe this system and its validation.

RESULTS AND DISCUSSION

Adapting the FUCCI Method to *Drosophila*

Although significant contributions to understanding the cell cycle and its regulation have been made using *Drosophila*, the FUCCI method had yet not been applied in this popular research organism. Geminin and Cdt1, the basic components of the original FUCCI system, show a high degree of sequence variability between species. This prompted us to employ an alternative strategy while developing a *Drosophila*-specific FUCCI system (referred to as Fly-FUCCI). Instead of Cdt1 the Fly-FUCCI system relies on the N-terminal part (aa 1–230) of *Drosophila* E2F1. This fragment contains the "PIP-box" degron that confers degradation by the S phase-dependent ubiquitin ligase CRL4^{Cdt2} (Shibutani et al., 2007, 2008), but which lacks the ability to bind DNA or activate target gene transcription (Figure 1B). In *Drosophila* S2 cells, GFP-E2F1$_{1–230}$ was degraded normally during S phase (Shibutani et al., 2008), and thus we decided to use E2F1$_{1–230}$ as a marker for cells in G2, M, and G1 phase.

The second probe of the original FUCCI system was based on the licensing inhibitor Geminin, which is degraded from midmitosis throughout G1 by the APC/C. Because ectopic expression of Geminin has a strong inhibitory effect on the cell cycle and can induce apoptosis (Quinn et al., 2001), we replaced Geminin with a degron from *Drosophila* Cyclin B (CycB). CycB promotes G2→M progression and, like Geminin, it is targeted for proteasomal degradation by APC/C (King et al., 1995). CycB proteolysis requires a conserved N-terminal 9 amino acid motif, termed the destruction box (D box). This motif can be transferred to heterologous proteins and render them APC/C targets (Glotzer

et al., 1991; King et al., 1996). Therefore, an N-terminal fragment (aa 1–266) of CycB including the D box was fused to mRFP1 to mark cells in S, G2, and M phase. Because this fragment lacks the cyclin box required for Cdk activation, overexpression of this construct should not affect the cell cycle (Figure 1B). Relative to the original FUCCI system applied in mammalian cell culture and transgenic mice, the Fly-FUCCI system has the advantage that it can clearly distinguish G1, S, and G2 phases. Moreover, because Fly-FUCCI uses an S phase-coupled, $CRL4^{Cdt2}$-dependent probe (GFP-$E2F1_{1–230}$) to detect G1→S transitions, it is much better for identifying S phase cells.

To validate the Fly-FUCCI system, we generated transgenic flies that constitutively expressed both Fly-FUCCI probes under control of the poly-*ubiquitin* promotor (Lee et al., 1988). Fluorescence-activated cell sorting (FACS) analysis of dissociated wing discs (Figure 1D) from these animals revealed high levels of green fluorescence in G1 and G2 cells, whereas the GFP signal was nearly absent from S phase cells. In contrast, red fluorescence was readily detected in cells in S, G2, or M phase, but not in cells with G1 DNA content. These observations demonstrate that simultaneous expression of both Fly-FUCCI probes allows accurate marking of all three categories of interphase cells: cells from anaphase to the G1→S transition are green, S phase cells are red, and cells in G2 and early mitosis are yellow (Figure 1A). Nevertheless, because the onset of probe degradation is easier to detect than the onset of probe accumulation, none of the probes used in any of the FUCCI systems can accurately place S→G2 transitions (the cessation of DNA replication). This can be done, however, by including a PCNA-based fusion protein, which localizes to distinct nuclear replication foci during S phases and disperses thereafter (Leonhardt et al., 2000; Lidsky et al., 2013).

The poly-*ubiquitin* promotor-driven Fly-FUCCI system has limited utility, however, because the analysis of cell proliferation in complex tissues often requires specific labeling of small subpopulations of cells. To overcome this limitation, we created transgenic flies (Figure 1C) expressing the Fly-FUCCI probes either under the original UASt promotor (Brand and Perrimon, 1993), or the weaker, germline-compatible UASp promotor (Rørth, 1998), or the QUAS promotor of the Q-system (Potter et al., 2010). These promotors can be activated in specific cell types by targeted expression of their respective transcriptional activators, Gal4 and Q-factor (QF). A plethora of Gal4 driver lines exist, including drivers specific for nearly every *Drosophila* cell type ever identified, and so Fly-FUCCI can be almost universally applied. With minor modifications, Fly-FUCCI can also be adapted for cell-cycle analysis in clonal lineages. To increase the spectrum of usable fluorophores, we created CFP- and Venus-based variants with the PIP box and D box degrons and these conditional promotors. These variants should enable complex experimental setups that include additional, red-fluorescent markers. The whole collection of Fly-FUCCI variants is available as recombinant stocks on the second and third chromosome (Table S1). Each combination of FUCCI probes can be detected by their native fluorescence without further amplification, but when using the weaker promotors (e.g., poly-*ubquitin* or UASp) a better signal-to-noise ratio can be achieved by staining with antibodies against GFP and RFP. In this regard, it is important to note that antibodies allowing faithful distinction of CFP and Venus were not available at the time of writing.

Expression of Fly-FUCCI Probes Does Not Affect Cell-Cycle Progression

To determine whether the Fly-FUCCI probes had any undesired effects on cell-cycle progression, they were expressed in the posterior compartments of larval wing imaginal discs using *hedgehog*-Gal4. To independently mark S or M phase cells, the wing discs were also labeled with either 5-ethynyl-2'-deoxyuridine (EdU) or an antibody recognizing phosphorylated Histone 3 (PH3). Cell division is evenly distributed throughout this single-layered epithelium, allowing a direct comparison of expressing and untreated cells in the posterior and anterior wing compartments, respectively. Expression of GFP-$E2F1_{1–230}$ or mRFP1-$CycB_{1–266}$ did not affect the pattern of EdU incorporation or PH3 staining (Figure S1), indicating that ectopic expression of the Fly-FUCCI system permits normal cell-cycle progression.

Fly-FUCCI Recapitulates Developmentally Programmed Cell-Cycle Patterns

To evaluate the effectiveness of the system, we tested whether expression of the Fly-FUCCI probes allows the visualization of developmentally programmed cell-cycle patterns. Wing imaginal disc cells proliferate in a mostly unpatterned fashion, but at the end of larval development a stripe of cells at the dorsoventral compartment boundary enter a developmentally programmed cell-cycle arrest (O'Brochta and Bryant, 1985), and therefore this region is referred to as the "zone of nonproliferating cells" (ZNC). The ZNC is subdivided into four domains (Johnston and Edgar, 1998): cells in the central region of the anterior portion as well as the whole posterior part of the ZNC undergo a G1 arrest, whereas the two outer cell rows of the anterior part stall in G2 phase (Figure 2A). Expression of the Fly-FUCCI system in late wing imaginal discs using the *sd*-Gal4 driver resulted in a distinct pattern within the EdU-negative cells of the ZNC (Figure 2B). As expected, GFP-$E2F1_{1–230}$ accumulated in all cells throughout the ZNC, whereas mRFP1-$CycB_{1–266}$ was absent in the posterior part, which is arrested in G1 phase. As predicted, the anterior region displayed two stripes of mRFP1-$CycB_{1–266}$-expressing cells, producing two narrow domains of double-positive G2 cells. Thus, we conclude that the Fly-FUCCI system can distinguish cells arrested in G1 from those in G2.

To evaluate whether the Fly-FUCCI system can also be utilized to visualize S phase cells, we extended our studies to eye-antenna discs. During the first two larval stages, eye imaginal disc cells proliferate in an unpatterned manner, but during the third instar differentiation begins. Photoreceptor cell differentiation is coordinated by the movement of the morphogenetic furrow (MF), which moves from posterior to anterior and thereby creates a distinct pattern of cell-cycle stages (reviewed in Baker, 2007). Undifferentiated cells anterior to the MF divide asynchronously; cells within the MF are synchronized in G1, and cells posterior to the MF initiate differentiation (Figure 2B). At this point, a subpopulation of cells exits the cell cycle in G1 and differentiates into photoreceptors, whereas the remaining cells execute a terminal cell cycle called the second mitotic wave (SMW). To determine whether the Fly-FUCCI system could

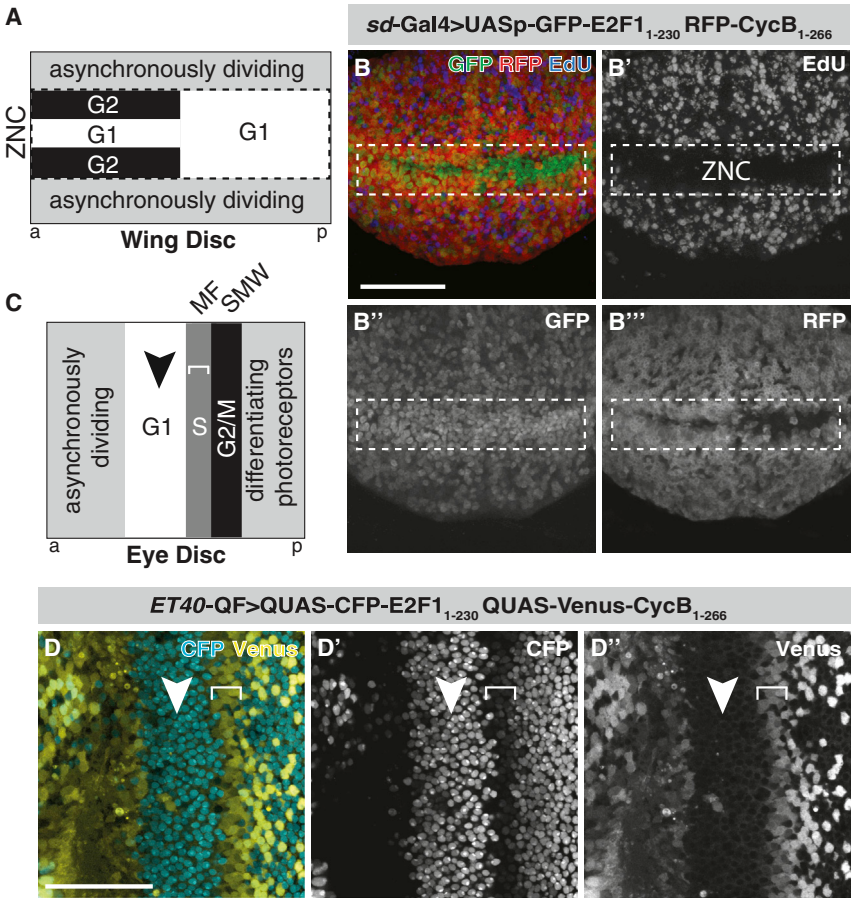

Figure 2. Fly-FUCCI Reveals Developmentally Regulated Cell-Cycle Patterns

(A and B) The Fly-FUCCI system enables the visualization of the patterned cell-cycle arrest of the zone of nonproliferating cells (ZNC). The cells in the center of the anterior part of the ZNC arrest in G1, whereas the adjacent cells undergo a G2 arrest. Cells in the posterior domain of the ZNC uniformly arrest in G1 (A). Wing disc-specific expression of the Fly-FUCCI system using the *scalloped*-Gal4 driver resulted in a distinctive pattern (B). The anterior part of the ZNC displayed a stripe of GFP-E2F1$_{1–230}$, flanked by narrow regions of yellow cells expressing both GFP-E2F1$_{1–230}$ and mRFP1-CycB$_{1–266}$. The posterior part of the ZNC, in contrast, showed uniform expression of GFP-E2F1$_{1–230}$. The ZNC (dashed line) was revealed in late larval wing imaginal discs by the absence of EdU (blue) incorporation (B″). GFP-E2F1$_{1–230}$ (green) and mRFP1-CycB$_{1–266}$ (red) were visualized by antibody staining. Scale bar, 50 μm.

(C and D) Cells in the posterior part of the disc divide asynchronously until they are synchronized in G1 by the anterior moving morphogenetic furrow (MF). The cells within the morphogenetic furrow subsequently separate into two subpopulations. One fraction of the G1-arrested cells terminates proliferation and immediately differentiates in photoreceptor cells, whereas the remaining cells enter a terminal cell cycle known as second mitotic wave (SMW). A CFP/YFP variant of the Fly-FUCCI system was expressed using the *ET40*-QF driver, which allows uniform expression of QUAS constructs throughout eye imaginal discs. In the asynchronously dividing anterior cells, both Fly-FUCCI probes were expressed in a salt and pepper pattern. Within the MF, the Venus-CycB$_{1–266}$ probe was absent, whereas CFP-E2F1$_{1–230}$ was readily detectable. All cells of SMW expressed high levels of the Venus-based probe, but CFP-E2F1$_{1–230}$ was degraded in a narrow stripe adjacent to the MF. The position of the MF is indicated by arrowheads. Brackets mark the S phase cells of the SMW. Scale bar, 50 μm.

visualize the linear arrangement of cell-cycle phases in eye imaginal discs, we employed the *ET40*-QF driver, which allows robust expression of QUAS constructs throughout the disc (Potter et al., 2010). *ET40*-QF-mediated overexpression of a CFP/Venus Fly-FUCCI variant resulted in a speckled pattern in the anterior, asynchronously cycling part of the eye disc (Figure 2D). The G1-arrested cells of the MF revealed high levels of CFP-E2F1$_{1–230}$ but were devoid of Venus-CycB$_{1–266}$. In contrast, Venus-CycB$_{1–266}$ was readily detectable in the narrow stripe posterior to the MF that represents the SMW. CFP-E2F1$_{1–230}$ was absent in the cells immediately posterior to the MF but subsequently reaccumulated resulting in a band of double-positive cells. This pattern is consistent with previous analyses showing that cells in the MF are synchronized in G1 but then undergo another S phase followed by a terminal mitosis (the SMW). Altogether, these experiments demonstrate that Fly-FUCCI is a very accurate tool for visualizing complex cell-cycle patterns in developing tissues.

Nuclear Targeting of the CycB-FUCCI Probe

GFP-E2F1$_{1–230}$ is present exclusively in the nucleus throughout the cell cycle, whereas RFP-CycB$_{1–266}$ is predominantly localized in the cytoplasm (Figure 3A). Although cytoplasmic localization can be advantageous because it allows the visualization of cell size or shape changes, it also complicates the recognition of the Fly-FUCCI probes during automated classification of cells, which is essential for applying the Fly-FUCCI method in any type of high-throughput format. Therefore, we modified the CycB-based probe by adding the nuclear localization signal (NLS) of SV40 large T antigen (Görlich and Mattaj, 1996). Fluorescence microscopy revealed that this fusion protein was efficiently targeted to the nucleus in S2-R$^+$ cells (Figure 3A). Moreover, Venus-NLS-CycB$_{1–266}$ expressed using the eye-disc-specific *ET40*-QF driver was degraded normally in the G1-arrested cells of the MF (Figure 3C), and FACS analysis of dissociated wing discs revealed a cell-cycle distribution identical to that of the initial Fly-FUCCI system (cf. Figure 3D and Figure 1D). Thus, nuclear targeting did not impair the functionality of the CycB-FUCCI probe.

Live Cell-Cycle Imaging in S2-R$^+$ Cells

Insect cell culture is increasingly important for high-throughput screening, prompting us to introduce the Fly-FUCCI method into S2-R$^+$ cells. However, our first attempts to generate stable S2-R$^+$ cells homogenously expressing the Fly-FUCCI probes failed, primarily because both probes were expressed from

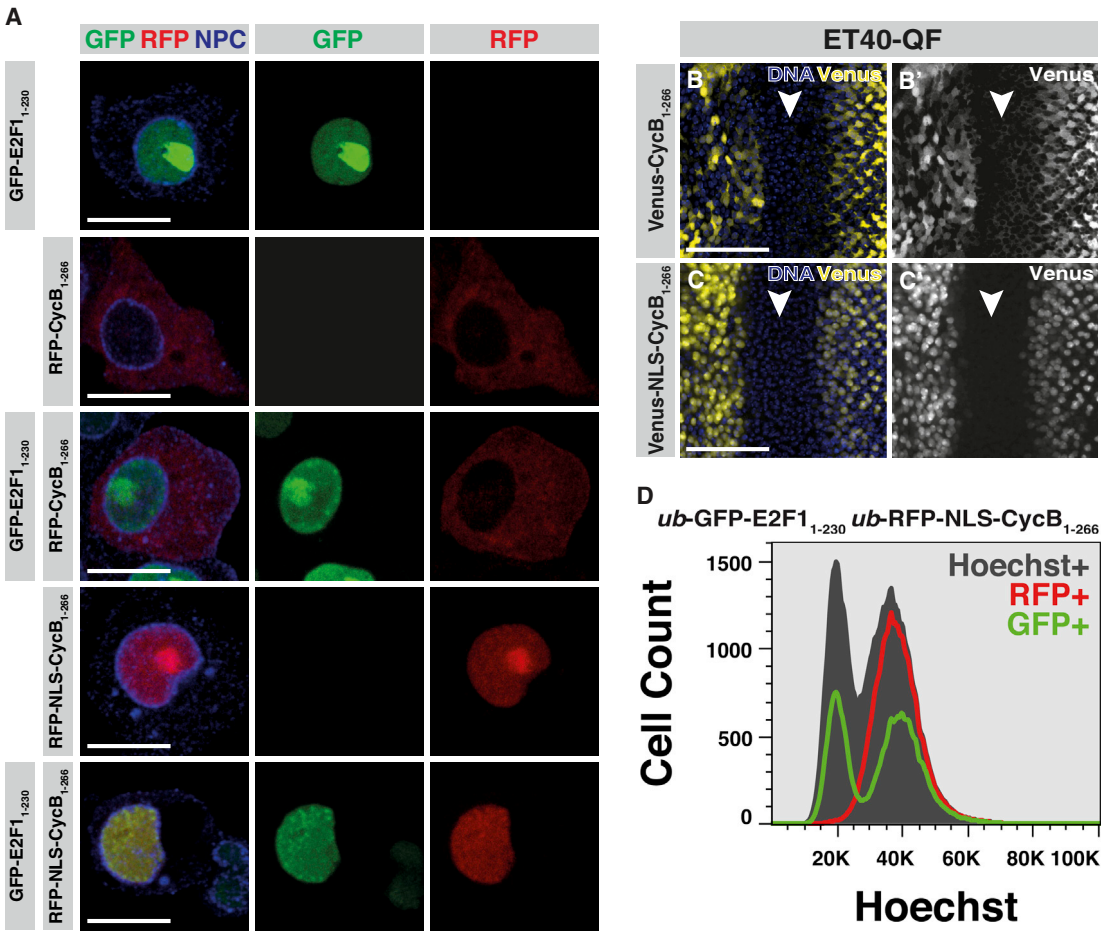

Figure 3. Nuclear Targeting of $CycB_{1–266}$

(A) Subcellular localization in S2-R^+ cells that were transfected with *act*-mRFP1-$CycB_{1–266}$ or *act*-mRFP1-NLS-$CycB_{1–266}$ (red), either alone or in combination with *act*-GFP-$E2F1_{1–230}$ (green). For better visualization, the cells were costained with an antibody against the nuclear core complex (NPC, blue). Normal mRFP1-$CycB_{1–266}$ was predominantly localized in the cytoplasm, but after fusion to a NLS the construct was exclusively found in the nucleus, and thus gives rise to "yellow" cells in conjunction with GFP-$E2F1_{1–230}$. Scale bars, 10 μm.

(B and C) Micrographs of eye imaginal discs expressing either QUAS-Venus-$CycB_{1–266}$ or QUAS-Venus-NLS-$CycB_{1–266}$ (yellow) under control of the *ET40*-QF driver. Both constructs were efficiently degraded in the G1-sychonronized cells of the morphogenetic furrow (arrowheads). DAPI (blue); scale bars, 50 μm.

(D) FACS profile of dissociated wing discs expressing *ub*-mRFP1-NLS-$CycB_{1–266}$ in combination with *ub*-GFP-$E2F1_{1–230}$. Most of the GFP-positive cells resided in G1 or G2 phase, whereas RFP expression was restricted to cells in S and G2 phase.

separate vectors that did not carry a selectable marker. To solve this problem, we designed a multicistronic vector that expresses both Fly-FUCCI probes and a neomycin resistance cassette as a single polypeptide (Figure 4A). The coding sequences of the individual components are separated by T2A sequences, a CHYSEL (*cis*-acting hydrolase element) peptide, which is derived from the insect virus *Thosea asigna* and effectively self-cleaves in *Drosophila* cells (González et al., 2011). This multicistronic construct allowed the selection of stable cell lines that express both components of the Fly-FUCCI system at equal levels. Inspection of these cells by FACS revealed three distinct populations of green, red, and yellow cells (Figure 4A), which correlated with the G1, S, and G2 peaks, respectively (Figures 4B and 4C). Moreover, colabeling with the nucleotide analog EdU showed that red fluorescence coincided with the execution of S phase (Figure 4D).

To observe the cell-cycle dynamics of the Fly-FUCCI system, we applied live microscopy to the FUCCI-labeled S2-R^+ cells (Figures 4E and 4F; Movie S1). Images were captured every 20 min for a period of 90 hr, allowing the recording of fluorescence intensities through multiple consecutive cell cycles. Consistent with data from fixed samples, high intensities of green and red fluorescence were followed by nuclear envelope breakdown and degradation of the red probe (mRFP1-NLS-$CycB_{1–166}$) during cell division. From this point, the intensity of the green signal (GFP-$E2F1_{1–230}$) steadily increased for 10 hr but then dropped dramatically, presumably when $CRL4^{Cdt2}$ is activated at the G1→S transition. After a short period (~1 hr) without a signal, we observed an increase in the red fluorescence intensity, followed by reaccumulation of the green probe after another 7 hr. Altogether, these findings indicate that the multicistronic Fly-FUCCI construct is functional in S2-R^+ cells.

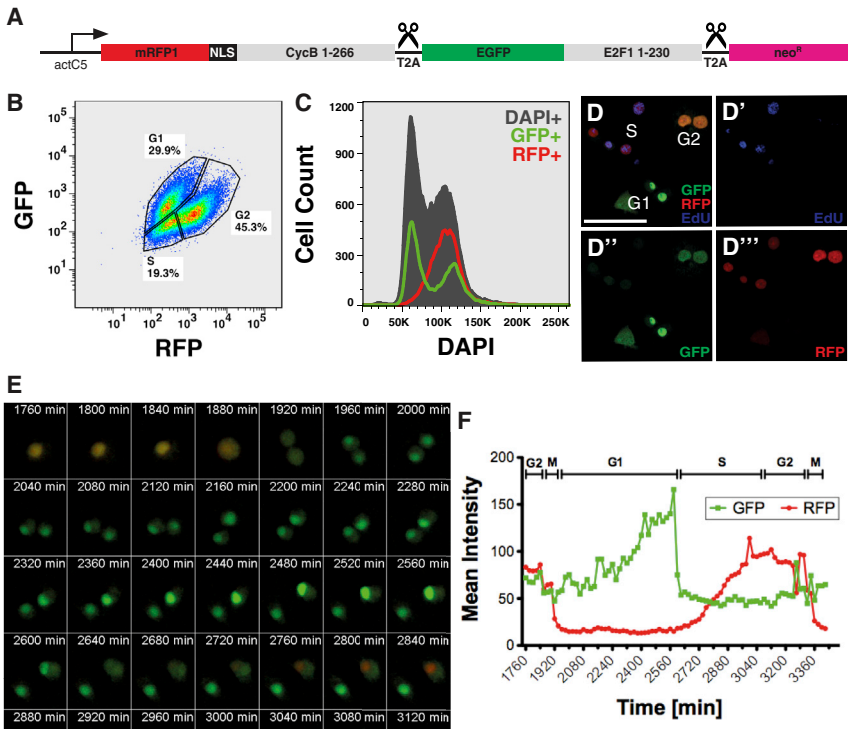

Figure 4. Fly-FUCCI Allows Real-Time Analysis of Cell-Cycle Phasing

(A) Schematic of the multicistronic Fly-FUCCI construct. mRFP1-CycB$_{1–266}$, GFP-E2F1$_{1–230}$, and neomycin resistance gene were expressed as a single polypeptide under control of the actin C5 promotor, whereby T2A autocleavage sites separate the individual components of the construct.

(B and C) Flowcytometric analysis of S2-R$^+$ cells expressing the multicistronic Fly-FUCCI construct. A scatterplot revealing three distinct populations of GFP-positive, RFP-positive, and double-positive cells (B). The corresponding cell-cycle profile showing a correlation between GFP expression and G1 and G2 phase as well as RFP expression and S and G2 phase.

(D) Micrographs of Fly-FUCCI-expressing S2-R$^+$ cells labeled with EdU (blue) and antibodies against GFP (green) or dsRed (red). Scale bar, 50 μm.

(E and F) Live imaging of Fly-FUCCI-expressing S2-R$^+$ cells. The image gallery in (E) shows the sequence of color changes that a cell undergoes during a whole cell cycle. Images were captured every 20 min. GFP is shown in green and RFP in red. Scale bar, 10 μm. The diagram in (F) shows a quantification of fluorescence intensities from the image sequence depicted in (E).

This should allow the design of complementary studies that combine cell-based screening with the powerful genetics of *Drosophila*.

Fly-FUCCI Robustly Detects Known Cell-Cycle Manipulations

Our data demonstrate that Fly-FUCCI can visualize cell-cycle oscillations in normal cells, but it remained unclear whether the system is sensitive enough to detect altered cell-cycle patterns. To address this question, we modulated the length of the G2 phase in the posterior compartments of developing wing discs by overexpressing either *string* (*stg*) or *Wee1* with the *hh*-Gal4 driver. To evaluate the sensitivity of the Fly-FUCCI system, dissociated wing discs of comparable genotype (*hh*-Gal4 was replaced by *en*-Gal4) were analyzed by FACS (Figure 5A). As previously reported (Neufeld et al., 1998), the Cdc25-type phosphatase Stg is rate limiting for entry into mitosis in *Drosophila* cells, and consequently ectopic expression of Stg/Cdc25 reduced the fraction of cells in G2 phase from 52.38% to 17.46%, whereas the number of cells in G1 concomitantly increased from 25.37% to 52.5%. Conversely, the overexpression of the inhibitory kinase *Wee1* increased the G2 cell population from 41.85% to 53.38% and decreased the G1 cells population from 25.13% to 18.69%. In agreement with these FACS data, wing discs carrying the Fly-FUCCI system exhibited increased numbers of green G1 cells upon overexpression of *stg* (Figure 5C) and an enrichment of yellow-labeled G2 cells after ectopic expression of *Wee1* (Figure 5D).

Similarly, we asked whether the FUCCI system could detect alterations in the duration of G1 phase. This can be achieved by ectopic expression of Cyclin E (CycE) or *dacapo (dap)* (Neufeld et al., 1998; Reis and Edgar, 2004). The transition from G1 to S phase relies on the activation of Cdk2 by CycE, and thus ectopic expression of CycE caused a decline of the G1 fraction from 26.84% to 14.54% and subsequent expansion of the G2 population from 34.54% to 56.37%. The Cyclin Kinase Inhibitor (CKI) *dap* restrains the activity of Cdk2, and therefore its misexpression resulted in the reverse phenotype: an increased number of G1 cells from 22.01% to 29.27% and a decreased G2 population from 35.39% to 31.41%. Consistently, the Fly-FUCCI system showed an enrichment of yellow G2 cells in the CycE-overexpressing region, whereas *dap* overexpression resulted in more green G1 cells. These data demonstrate that the Fly-FUCCI system can detect alterations in cell-cycle progression, and that the resulting cell-cycle distributions are comparable to data obtained by flow cytometry.

Fly-FUCCI-Imaging in Specific Cell Types in the Adult Midgut

The intestinal epithelium of the adult fly midgut is maintained by intestinal stem cells (ISCs) that grow on a sheath of visceral muscle and generate two major types of differentiated progeny, enterocytes (EC) and enteroendocrine (EE) cells (Figure 6A; reviewed in Jiang and Edgar, 2012). Altogether, the midgut comprises at least six major cell types and is several cell layers thick,

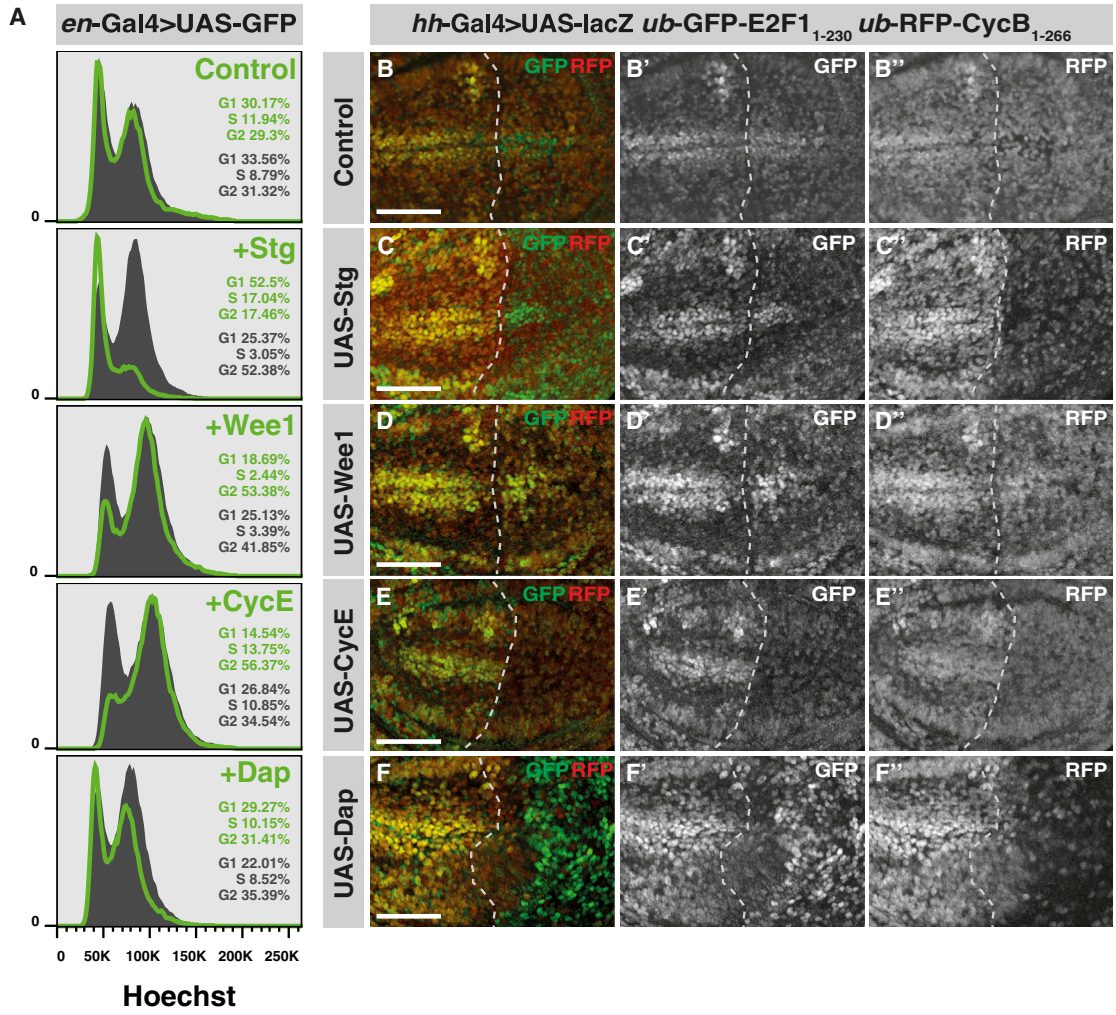

Figure 5. Fly-FUCCI Reveals Altered Cell Cycles in Wing Discs

(A) FACS profiles of dissociated wing imaginal discs overexpressing the indicated cell-cycle regulators and GFP. The *engrailed*-Gal4 was used to direct the overexpression of the UAS constructs to the posterior compartment, thus allowing a direct comparison with untreated, GFP-negative cells.

(B–F) Overexpression of the same set of cell-cycle regulators in wing imaginal discs coexpressing the Fly-FUCCI system (*ub*-GFP-E2F1$_{1–230}$ *ub*-mRFP1-NLS-CycB$_{1–266}$). Overexpression in the posterior compartment was achieved with *hh*-Gal4 and indicated by lacZ staining. A dashed line marks the anterior-posterior compartment border. The Fly-FUCCI probes were visualized by staining with antibodies against GFP (green) or dsRed (red). Scale bar, 50 μm.

which complicates accurate high-resolution imaging. To further validate the Fly-FUCCI system, we investigated whether it was capable of assessing the cell-cycle properties of each of three different cell types in this complex tissue.

We first expressed the Fly-FUCCI probes with the ISC-specific driver *Delta*-Gal4 (Zeng et al., 2010). ISCs are the only mitotically active cells in the midgut, and their proliferation can be greatly stimulated by damaging the gut epithelium, for instance, by enteric infection with *Pseudomonas entomophila* (*P.e.*) (Jiang and Edgar, 2012). In agreement with FACS analysis (Figure 6B), the Fly-FUCCI system showed that quiescent Delta$^+$ ISCs in healthy animals are normally arrested in either G1 (~55%) or G2 (~45%) (Figures 6C and 6E). Costaining with antibodies against Delta, which exhibits more dynamic expression than *Dl*-Gal4, indicated cells actively expressing Delta reside predominantly in G2 (~60%) (Figure S3). Activating ISC proliferation by *P.e.* infection increased the fraction of ISCs with S phase and G2 Fly-FUCCI expression patterns and decreased the G1 fraction from 55% to 20% ($p < 0.0001$, Student's t test). The S and G2/M fractions increased accordingly to 8% ($p < 0.01$) and 70% ($p < 0.0001$) (Figure 6E). Thus, the Fly-FUCCI system could easily detect the transition from quiescence to proliferation in this stem cell population.

We next assessed Fly-FUCCI readouts in postmitotic, differentiated enteroendocrine (EE) cells, which FACS analysis showed to be arrested in G1 (Figure 7D). Using the EE-specific *pros*^{v1}-Gal4 driver (Figure 7C), we discovered that G1-arrested EEs have low levels of not only CRL4^{Cdt2} activity, but also APC/C activity (Figures 7A and 7B). This is an unusual state, because most terminally differentiated cells are believed to exit

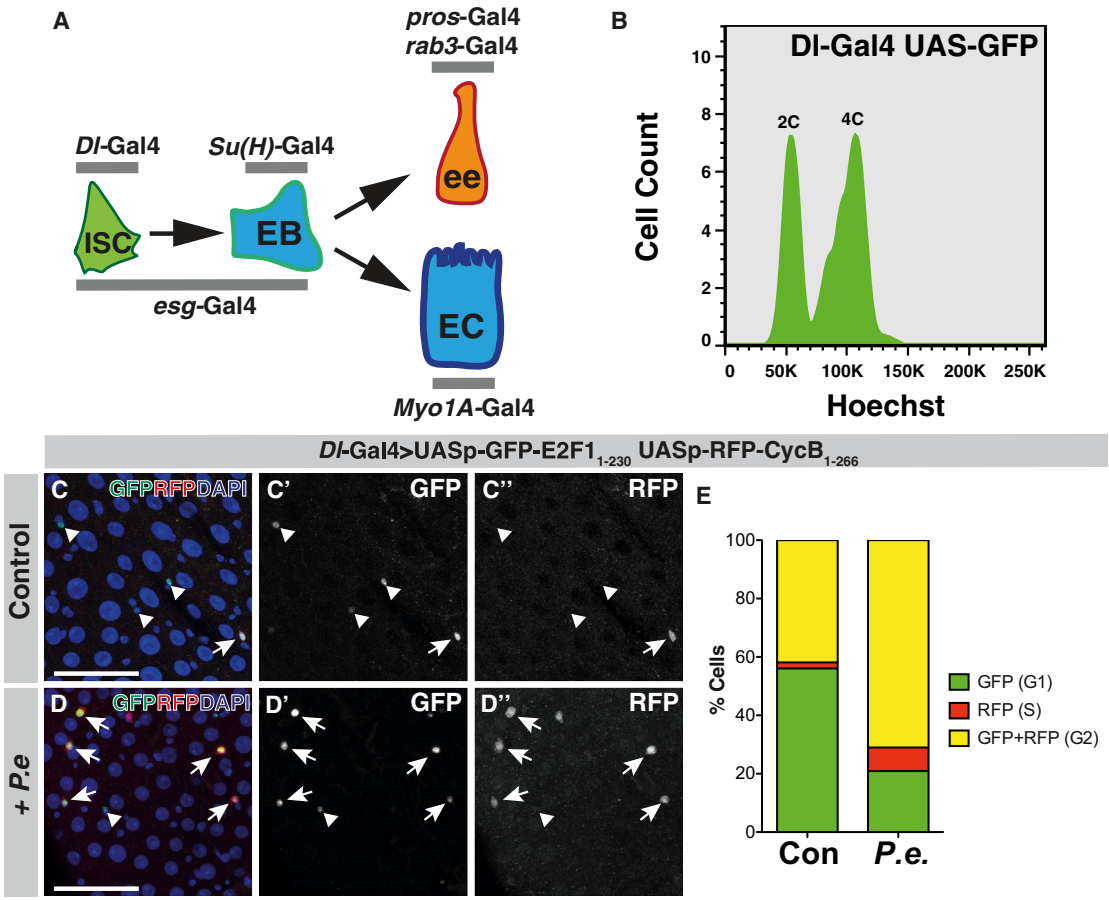

Figure 6. ISCs Can Arrest in Different Phases of the Cell Cycle

(A) Schematic representation of the *Drosophila* intestinal stem cell lineage with the different drivers used to examine Fly-FUCCI distribution in all midgut cell types.

(B) Cell-cycle distribution of ISCs determined by FACS profiling of *Dl*-Gal4 > UAS-GFP midguts.

(C and D) Fly-FUCCI cell-cycle distribution of *Dl*-Gal4 > UASp-GFP-E2F1$_{1–230}$ UASp-mRFP1-CycB$_{1–266}$ midguts under homeostatic conditions (Con) (C) and upon *P.e*. infection (*P.e*.) (D). Arrows indicate cells in G2; arrowheads indicate cells in G1. The Fly-FUCCI probes were visualized by staining with antibodies against GFP (green) or dsRed (red). Scale bars, 50 μm.

(E) Quantification of genotypes in (C) and (D).

the cell cycle in a G1 or G0 state characterized by high APC/C activity (Buttitta et al., 2010; Ruggiero et al., 2012; Tanaka-Matakatsu et al., 2007). Furthermore, our analysis revealed that a few EEs displayed an S phase Fly-FUCCI pattern (Figure 7A, arrowhead, B). Immunostaining for PH3 and incorporated EdU confirmed that these cells were indeed actively cycling EEs (Figure S4). This observation suggests that EEs can occasionally progress through at least one mitotic cycle after they have initiated differentiation.

We next used the *MyoIA*-Gal4 driver to drive Fly-FUCCI expression in differentiated enterocytes (ECs) (Figure 7F). These cells undergo several endocycles as part of their differentiation process and terminally arrest in an endocycle gap phase with C values in the 8–32C range (Figure 7E). Interestingly, the Fly-FUCCI probes revealed that ECs arrest with low CRL4^{Cdt2} and high APC/C activity and are therefore in a G1-like state rather different from that observed in terminally arrested EEs (Figure 7F). Finally, we assayed Fly-FUCCI probe expression in young, endocycling ECs generated following an enteric infection with *P.e.* In this case, the Fly-FUCCI system revealed a dramatic induction of the APC/C-sensitive mRFP1-CycB$_{1–166}$ probe, reflecting the periodic suppression of APC/C activity that occurs during endocycle S phases (reviewed in Zielke et al., 2013) (Figure S2). Endocycling ECs also displayed periodic loss of the CRL4^{Cdt2}-sensitive GFP-E2F1$_{1–230}$ probe during S phases, as revealed by costaining for incorporated EdU (Figure 7G, arrowheads). Thus, the Fly-FUCCI system can easily distinguish endocycling from arrested ECs. Overall, these observations indicate that the Fly-FUCCI system can be effectively used to detect a number of unique cell-cycle properties in specific subpopulations of cells, even in a complex tissue context.

The invention of the Fly-FUCCI system has several implications for the design of future studies on cell proliferation. First, the Fly-FUCCI system might be capable of revealing subtle cell-cycle changes, and thus it could be used as a reporter during screening approaches. Tellingly, this strategy was recently employed in a screen for small molecules involved in cardiomyocyte regeneration in zebrafish (Choi et al., 2013). Second, Fly-FUCCI

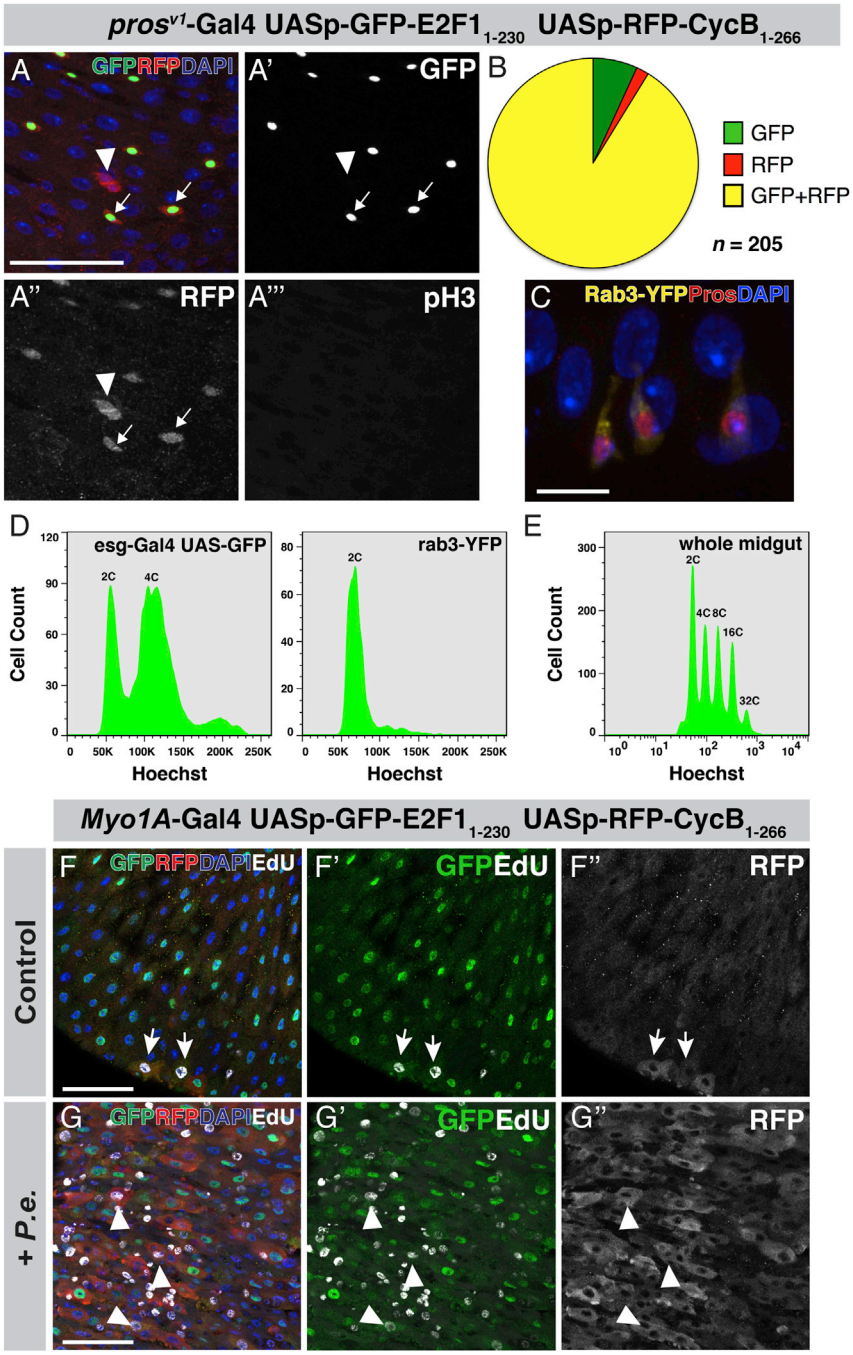

Figure 7. Differentiated Midgut Cells Can Arrest with APC/C Either On or Off

(A) Cell-cycle distribution of EE cells was determined by examining *pros*^{v1}-Gal4 > UASp-GFP-E2F1$_{1–230}$ UASp-mRFP1-CycB$_{1–266}$ under homeostatic conditions. Confocal images of *pros*^{v1}-Gal4 > UASp-GFP-E2F1$_{1–230}$ UASp-mRFP1-CycB$_{1–266}$ animals. The arrowhead in (A) indicates a rare S phase occurrence in the posterior midgut, where most of the EEs arrest with low APC activity (A, arrows). The Fly-FUCCI probes were visualized by staining with antibodies against GFP (green) or dsRed (red). Scale bars, 50 μm.

(B) Quantification of (A).

(C) The *Rab3*-YFP reporter (Yellow) marks Pros-positive (Red) EE cells. Scale bar, 10 μm.

(D) FACS profiles for the ISC+EB population (*esg*-Gal4 > UAS-GFP, left) and EE cells (*Rab3*-YFP, right). Hoechst staining intensity is on the x axis; cell counts are on the y axis.

(E) FACS profile of the entire midgut. Hoechst staining intensity peaks show the EC population as several peaks with a >4C DNA content.

(F and G) Fly-FUCCI expression pattern for enterocytes under homeostatic (F) and *P.e.*-infected (G) conditions. We used the *MyoIA*^{NP0001}-Gal4 to drive UASp-GFP-E2F1$_{1–230}$ UASp-mRFP1-CycB$_{1–266}$ in differentiated ECs and performed EdU incorporation on both control and infected midguts for 2 hr. (F) Control midguts under homeostatic conditions are marked by the absence of the mRFP1-CycB$_{1–266}$ probe, except for rare S phase cells that also incorporate EdU (F, arrows). (G) Many EC cells in *P.e.*-infected midguts have high levels of the mRFP1-CycB$_{1–266}$ probe as well as an increase in the number of EdU-positive cells (E, arrowheads). Note that none of the EdU-positive cells in (F) and (G) have significant levels of the GFP-E2F1$_{1–230}$ probe present (F and G, arrows/arrowheads). The Fly-FUCCI probes were visualized by staining with antibodies against GFP (green) or dsRed (red). Scale bars, 50 μm.

enables the researcher to use FACS to isolate genetically defined subsets of actively proliferating cells, which could then be used for further assays such as profiling of gene expression or metabolic markers. Consistent with this idea, a recent publication reported the generation of transcriptional profiles from replicating hepatocytes that were purified with the help of a CycB-based reporter (Klochendler et al., 2012). In summary, the Fly-FUCCI system represents a widely applicable toolkit for the real-time analysis of cell-cycle oscillations and hence advances the design of functional studies and high-content screening approaches.

EXPERIMENTAL PROCEDURES

Molecular Cloning

The entry clone pENTR-E2F1$_{1–230}$ (Shibutani et al., 2008) was combined with the destination vectors pAGW, pUGW, pTGW, pPGW, pTCW, and pPCW of the *Drosophila* Gateway Collection (DGRC) as well as the newly generated Q system-compatible vectors pQGW and pQCW. The region corresponding to amino acids 1–266 of CycB were amplified by PCR using the primers CACCATGGTGGGCACAA CACTG, GCTCCAGCTCCACCTGCTACAAG and subsequently subcloned into the pENTR-D-TOPO Vector (Invitrogen). NLS-CycB$_{1–266}$ was generated by inserting a synthetic fragment containing the NLS of the SV40 large T antigen (PKKKRKV; Görlich and Mattaj, 1996) into pENTR-CycB$_{1–266}$ using the BanI/ApaI restriction sites. pENTR-CycB$_{1–266}$ and pENTR-NLS-CycB$_{1–266}$ were then combined with the destination vectors pARW, pURW, pTRW, pPRW, pTVW, pPVW (*Drosophila* Gateway Collection, DGRC), as well as the custom-made vectors pQRW and pQCW. The Q system-compatible vectors

(pQGW, pQRW, pQCW, and pQVW) were generated by subcloning of the tag-containing Gateway cassettes from the corresponding pUASp vectors into pQUAS (Potter et al., 2010). The multicistronic FUCCI vector (pAc5-GFP-E2F1$_{1–230}$-T2A-mRFP1-NLS-CycB$_{1–266}$-T2A-neo) was created by subcloning of synthetic Fly-FUCCI fragments into pAC5-Stable2 (González et al., 2011) using the Xba1/HindIII and KpnI/NotI restriction sites.

Fly Husbandry

Transgenic FUCCI flies were created by P-element-mediated transformation of w^{1118} embryos (Genetic Services). Recombinant flies coexpressing GFP/RFP or CFP/Venus variants of the Fly-FUCCI system on either second or third chromosome were selected by darker eye color and subsequently verified by PCR using the Phire Animal Tissue Direct PCR Kit (Thermo Scientific) and the following primer pairs: AAGGGCGAGGAGCTGTTCA, TCGTCCATGCCGAGAGTGAT (GFP-E2F1$_{1–230}$); AGGACGTCATCAAGGAGTTCA, TTGACCTCGGCGTCGTAGT (mRFP1-CycB$_{1–266}$); CGACCACTACCAGCAGAACA, TGCTCAGGACGTGATCGTAG (CFP-E2F1$_{1–230}$); ACGTCTATATCACCGCCGAC, TTGAAGTTCTCCGAAGCGTT (Venus-CycB$_{1–266}$). Mutant or transgene fly stocks were described elsewhere: *hh*-Gal4 (Tanimoto et al., 2000); *sd*-Gal4 (Bloomington, BL#8609); ET40-QF (Potter et al., 2010); *esg*^{NP7397}-Gal4 (Jiang and Edgar, 2009); *MyoIA*^{NP0001}-Gal4 (Jiang and Edgar, 2009); *pros*^{V1}-Gal4; Rab3-YFP (Chan et al., 2011); *Dl*-Gal4 (Zeng et al., 2010); UAS-Stg (Neufeld et al., 1998); UAS-Cyclin E (Neufeld et al., 1998); UAS-Wee1 (Reis and Edgar, 2004); UAS-DapIII.4 (Reis and Edgar, 2004).

Cell Culture

S2-R$^+$ cells were cultivated at 25°C in Schneider's Medium (Invitrogen) supplemented with 10% fetal calf serum, 100 U/ml penicillin, and 100 μg/ml streptomycin. For the generation of stable lines, cells were transfected with the Calcium Phosphate Transfection kit (Invitrogen). For the analysis of subcellular localization pAGW-E2F1$_{1–230}$, pARW-CycB$_{1–266}$, or pARW-NLS-CycB$_{1–266}$ were cotransfected with pCoHygro (Invitrogen) and selected for 4–6 weeks with 10 μg/ml Hygromycin B (Invitrogen). Cells stably expressing pAc5-GFP-E2F1$_{1–230}$-T2A-mRFP1-NLS-CycB$_{1–266}$-T2A-neo were selected for 4–6 weeks with 2 mg/ml Geneticin (Invitrogen) and afterward enriched by FACS sorting to generate a homogenous culture.

Immunohistochemistry

Wing or eye imaginal discs from wandering larvae were dissected in PBS and fixed for 30 min in 4% paraformaldehyde/PBS. Midguts were dissected from adult females (aged 3–7 days at 25°C) and were fixed for 30 min in 4% paraformaldehyde/PBS. For immunostaining S2-R$^+$ cells were seeded in μ-Slides 8 well (Ibidi) and fixed for 30 min in 4% paraformaldehyde/PBS. For EdU labeling, cells or dissected tissues, were incubated for 1–2 hr with EdU (1:1,000); fixed for 30 min in 4% paraformaldehyde/PBS, and processed according to the manual of the Click-It EdU Alexa Fluor 647 imaging kit (Invitrogen). Primary antibodies were used in the following dilutions: chicken anti-GFP (1:500, Invitrogen); rabbit anti-DsRed (1:500, Clontech); mouse anti-Nuclear Pore Complex (1:5,000, Abcam); mouse anti-Delta (extracellular domain) (1:50, Developmental Studies Hybridoma Bank); mouse anti-β-Gal (1:500, Sigma-Aldrich). Secondary antibodies, coupled to various Alexa dyes (Invitrogen), were used at a dilution of 1:2,000. DNA was visualized with 0.5 μg/ml DAPI (Sigma-Aldrich). Stained tissues were mounted in Vectashield (Vector Labs), except EdU-labeled samples, which were mounted in ProLong Gold Antifade (Invitrogen). Images of fixed samples were acquired on a Leica SP5 II confocal and processed with Fiji (http://fiji.sc/Fiji).

Pseudomonas entomophila Infection

P.e. culture was grown overnight at 31°C in Luria-Bertani medium supplemented with Rifampicin. The following day, *P.e.* culture was centrifuged at 4,000 rpm for 15 min, and the pelleted bacteria was resuspended in 5 ml of 2% sucrose-solution. Five hundred microliters of this solution was stirred through normal food, and flies were subsequently transferred to 29°C. Control flies were kept on normal food after transfer to 29°C. After 48 hr of infection, midguts were dissected and stained as described above. Image quantification data were acquired from duplicate control and *P.e.*-infected samples of 12–15 midguts each.

Midgut Cell Quantification

Fly-FUCCI positive cells were counted manually using Fiji (http://fiji.sc/Fiji). Between 10 and 15 ROIs from the anterior and posterior sections of the midgut, each approximately 500 μm^2, were counted out per driver line and condition. For the Fly-FUCCI quantification of Delta-positive cells, a total of 280 cells from seven different ROIs from five different posterior midguts were analyzed. Data were analyzed and tested for significance using the Student's t test in Prism5 (GraphPad).

Flow Cytometry

Cell-cycle profiles of wing imaginal discs were generated according to de la Cruz and Edgar (2008). Approximately 30 wing imaginal discs were dissected in PBS from third instar larvae and subsequently dissociated for 3–4 hr in 10× Trypsin-EDTA (Sigma) supplemented with 0.5 μg/ml Hoechst 33342. For cell-cycle analysis of S2-R$^+$ cells, we followed the protocol of Darzynkiewicz et al. (2001). In brief, cells were harvested by Trypsin-EDTA treatment, fixed for at least 2 hr in cold 70% EtOH, and finally stained with 1 μg/ml DAPI in PBS supplemented with 0.1% Triton X-100. Flow cytometry was performed on either a FACS Arias II or a FACS Canto II Instrument (both Becton Dickinson), and the resulting data were analyzed with FlowJo 7.6.2 (Tree Star).

Live Imaging

For real-time analysis, 1 × 10^5 cells were seeded in 35 mm μ-dishes (Ibidi). A time series of z stacks (2 μm slices) were captured every 20 min for an overall time frame of 90 hr on an Olympus Cell-R imaging system equipped with an Orca-R2 CCD Camera (Hamamatsu) and a 20× NA0.75 objective. The intensity of the green and red fluorescence signal was quantified from max projections using Fiji (http://fiji.sc/Fiji).

SUPPLEMENTAL INFORMATION

Supplemental Information includes four figures, one table, and one movie and can be found with this article online at http://dx.doi.org/10.1016/j.celrep.2014.03.020.

ACKNOWLEDGMENTS

We are grateful to R.J. Duronio, C. Lehner, F. Sprenger, T. Klein, J. de Navascues, M. Brankatschk, S. Hou, and the Developmental Studies Hybridoma Bank for providing reagents. We also thank C. Hoerth and H. Lorenz in the ZMBH imaging core, M. Langlotz in the ZMBH FACS core, and J. Pouch for technical assistance. An Intramural Young Investigator Grant (K-215) from the DKFZ supported the work of N.Z.; J.K. was supported by an EMBO Long-Term Fellowship. Funding in the Edgar lab was provided by ERC Advanced grant 268515, the DKFZ, and DFG SFB 873.

Received: December 3, 2013
Revised: February 6, 2014
Accepted: March 7, 2014
Published: April 10, 2014

REFERENCES

Arias, E.E., and Walter, J.C. (2006). PCNA functions as a molecular platform to trigger Cdt1 destruction and prevent re-replication. Nat. Cell Biol. *8*, 84–90.

Baker, N.E. (2007). Patterning signals and proliferation in Drosophila imaginal discs. Curr. Opin. Genet. Dev. *17*, 287–293.

Brand, A.H., and Perrimon, N. (1993). Targeted gene expression as a means of altering cell fates and generating dominant phenotypes. Development *118*, 401–415.

Buttitta, L.A., Katzaroff, A.J., and Edgar, B.A. (2010). A robust cell cycle control mechanism limits E2F-induced proliferation of terminally differentiated cells in vivo. J. Cell Biol. *189*, 981–996.

Calder, A., Roth-Albin, I., Bhatia, S., Pilquil, C., Lee, J.H., Bhatia, M., Levadoux-Martin, M., McNicol, J., Russell, J., Collins, T., and Draper, J.S. (2013).

Lengthened G1 phase indicates differentiation status in human embryonic stem cells. Stem Cells Dev. *22*, 279–295.

Chan, C.C., Scoggin, S., Wang, D., Cherry, S., Dembo, T., Greenberg, B., Jin, E.J., Kuey, C., Lopez, A., Mehta, S.Q., et al. (2011). Systematic discovery of Rab GTPases with synaptic functions in Drosophila. Curr. Biol. *21*, 1704–1715.

Choi, W.Y., Gemberling, M., Wang, J., Holdway, J.E., Shen, M.C., Karlstrom, R.O., and Poss, K.D. (2013). In vivo monitoring of cardiomyocyte proliferation to identify chemical modifiers of heart regeneration. Development *140*, 660–666.

Coronado, D., Godet, M., Bourillot, P.Y., Tapponnier, Y., Bernat, A., Petit, M., Afanassieff, M., Markossian, S., Malashicheva, A., Iacone, R., et al. (2013). A short G1 phase is an intrinsic determinant of naïve embryonic stem cell pluripotency. Stem Cell Res. *10*, 118–131.

Darzynkiewicz, Z., Juan, G., and Bedner, E. (2001). Determining cell cycle stages by flow cytometry. Curr. Protoc. Cell Biol., Chapter 8, Unit 84. http://dx.doi.org/10.1002/0471143030.cb0804s01.

Davoli, T., and de Lange, T. (2012). Telomere-driven tetraploidization occurs in human cells undergoing crisis and promotes transformation of mouse cells. Cancer Cell *21*, 765–776.

Davoli, T., Denchi, E.L., and de Lange, T. (2010). Persistent telomere damage induces bypass of mitosis and tetraploidy. Cell *141*, 81–93.

de la Cruz, A.F., and Edgar, B.A. (2008). Flow cytometric analysis of Drosophila cells. Methods Mol. Biol. *420*, 373–389.

Glotzer, M., Murray, A.W., and Kirschner, M.W. (1991). Cyclin is degraded by the ubiquitin pathway. Nature *349*, 132–138.

González, M., Martín-Ruíz, I., Jiménez, S., Pirone, L., Barrio, R., and Sutherland, J.D. (2011). Generation of stable Drosophila cell lines using multicistronic vectors. Sci. Rep. *1*, 75.

Görlich, D., and Mattaj, I.W. (1996). Nucleocytoplasmic transport. Science *271*, 1513–1518.

Jiang, H., and Edgar, B.A. (2009). EGFR signaling regulates the proliferation of Drosophila adult midgut progenitors. Development *136*, 483–493.

Jiang, H., and Edgar, B.A. (2012). Intestinal stem cell function in Drosophila and mice. Curr. Opin. Genet. Dev. *22*, 354–360.

Johnston, L.A., and Edgar, B.A. (1998). Wingless and Notch regulate cell-cycle arrest in the developing Drosophila wing. Nature *394*, 82–84.

King, R.W., Peters, J.M., Tugendreich, S., Rolfe, M., Hieter, P., and Kirschner, M.W. (1995). A 20S complex containing CDC27 and CDC16 catalyzes the mitosis-specific conjugation of ubiquitin to cyclin B. Cell *81*, 279–288.

King, R.W., Glotzer, M., and Kirschner, M.W. (1996). Mutagenic analysis of the destruction signal of mitotic cyclins and structural characterization of ubiquitinated intermediates. Mol. Biol. Cell *7*, 1343–1357.

Kleiblova, P., Shaltiel, I.A., Benada, J., Ševčík, J., Pecháčková, S., Pohlreich, P., Voest, E.E., Dundr, P., Bartek, J., Kleibl, Z., et al. (2013). Gain-of-function mutations of PPM1D/Wip1 impair the p53-dependent G1 checkpoint. J. Cell Biol. *201*, 511–521.

Klochendler, A., Weinberg-Corem, N., Moran, M., Swisa, A., Pochet, N., Savova, V., Vikeså, J., Van de Peer, Y., Brandeis, M., Regev, A., et al. (2012). A transgenic mouse marking live replicating cells reveals in vivo transcriptional program of proliferation. Dev. Cell *23*, 681–690.

Lee, H.S., Simon, J.A., and Lis, J.T. (1988). Structure and expression of ubiquitin genes of Drosophila melanogaster. Mol. Cell. Biol. *8*, 4727–4735.

Leonhardt, H., Rahn, H.P., Weinzierl, P., Sporbert, A., Cremer, T., Zink, D., and Cardoso, M.C. (2000). Dynamics of DNA replication factories in living cells. J. Cell Biol. *149*, 271–280.

Lidsky, P.V., Sprenger, F., and Lehner, C.F. (2013). Distinct modes of centromere protein dynamics during cell cycle progression in Drosophila S2R+ cells. J. Cell Sci. *126*, 4782–4793.

McGarry, T.J., and Kirschner, M.W. (1998). Geminin, an inhibitor of DNA replication, is degraded during mitosis. Cell *93*, 1043–1053.

Nasmyth, K. (2001). A prize for proliferation. Cell *107*, 689–701.

Neufeld, T.P., de la Cruz, A.F., Johnston, L.A., and Edgar, B.A. (1998). Coordination of growth and cell division in the Drosophila wing. Cell *93*, 1183–1193.

Nishitani, H., Sugimoto, N., Roukos, V., Nakanishi, Y., Saijo, M., Obuse, C., Tsurimoto, T., Nakayama, K.I., Nakayama, K., Fujita, M., et al. (2006). Two E3 ubiquitin ligases, SCF-Skp2 and DDB1-Cul4, target human Cdt1 for proteolysis. EMBO J. *25*, 1126–1136.

O'Brochta, D.A., and Bryant, P.J. (1985). A zone of non-proliferating cells at a lineage restriction boundary in Drosophila. Nature *313*, 138–141.

Ogura, Y., Sakaue-Sawano, A., Nakagawa, M., Satoh, N., Miyawaki, A., and Sasakura, Y. (2011). Coordination of mitosis and morphogenesis: role of a prolonged G2 phase during chordate neurulation. Development *138*, 577–587.

Pauklin, S., and Vallier, L. (2013). The cell-cycle state of stem cells determines cell fate propensity. Cell *155*, 135–147.

Potter, C.J., Tasic, B., Russler, E.V., Liang, L., and Luo, L. (2010). The Q system: a repressible binary system for transgene expression, lineage tracing, and mosaic analysis. Cell *141*, 536–548.

Quinn, L.M., Herr, A., McGarry, T.J., and Richardson, H. (2001). The Drosophila Geminin homolog: roles for Geminin in limiting DNA replication, in anaphase and in neurogenesis. Genes Dev. *15*, 2741–2754.

Reis, T., and Edgar, B.A. (2004). Negative regulation of dE2F1 by cyclin-dependent kinases controls cell cycle timing. Cell *117*, 253–264.

Roccio, M., Schmitter, D., Knobloch, M., Okawa, Y., Sage, D., and Lutolf, M.P. (2013). Predicting stem cell fate changes by differential cell cycle progression patterns. Development *140*, 459–470.

Rørth, P. (1998). Gal4 in the Drosophila female germline. Mech. Dev. *78*, 113–118.

Ruggiero, R., Kale, A., Thomas, B., and Baker, N.E. (2012). Mitosis in neurons: Roughex and APC/C maintain cell cycle exit to prevent cytokinetic and axonal defects in Drosophila photoreceptor neurons. PLoS Genet. *8*, e1003049.

Sakaue-Sawano, A., Kurokawa, H., Morimura, T., Hanyu, A., Hama, H., Osawa, H., Kashiwagi, S., Fukami, K., Miyata, T., Miyoshi, H., et al. (2008). Visualizing spatiotemporal dynamics of multicellular cell-cycle progression. Cell *132*, 487–498.

Sakaue-Sawano, A., Kobayashi, T., Ohtawa, K., and Miyawaki, A. (2011). Drug-induced cell cycle modulation leading to cell-cycle arrest, nuclear mis-segregation, or endoreplication. BMC Cell Biol. *12*, 2.

Santos, S.D., Wollman, R., Meyer, T., and Ferrell, J.E., Jr. (2012). Spatial positive feedback at the onset of mitosis. Cell *149*, 1500–1513.

Shibutani, S., Swanhart, L.M., and Duronio, R.J. (2007). Rbf1-independent termination of E2f1-target gene expression during early Drosophila embryogenesis. Development *134*, 467–478.

Shibutani, S.T., de la Cruz, A.F., Tran, V., Turbyfill, W.J., 3rd, Reis, T., Edgar, B.A., and Duronio, R.J. (2008). Intrinsic negative cell cycle regulation provided by PIP box- and Cul4Cdt2-mediated destruction of E2f1 during S phase. Dev. Cell *15*, 890–900.

Son, S., Tzur, A., Weng, Y., Jorgensen, P., Kim, J., Kirschner, M.W., and Manalis, S.R. (2012). Direct observation of mammalian cell growth and size regulation. Nat. Methods *9*, 910–912.

Spencer, S.L., Cappell, S.D., Tsai, F.C., Overton, K.W., Wang, C.L., and Meyer, T. (2013). The proliferation-quiescence decision is controlled by a bifurcation in CDK2 activity at mitotic exit. Cell.

Sugiyama, M., Sakaue-Sawano, A., Iimura, T., Fukami, K., Kitaguchi, T., Kawakami, K., Okamoto, H., Higashijima, S., and Miyawaki, A. (2009). Illuminating cell-cycle progression in the developing zebrafish embryo. Proc. Natl. Acad. Sci. USA *106*, 20812–20817.

Tanaka-Matakatsu, M., Thomas, B.J., and Du, W. (2007). Mutation of the Apc1 homologue shattered disrupts normal eye development by disrupting G1 cell cycle arrest and progression through mitosis. Dev. Biol. *309*, 222–235.

Tanimoto, H., Itoh, S., ten Dijke, P., and Tabata, T. (2000). Hedgehog creates a gradient of DPP activity in Drosophila wing imaginal discs. Mol. Cell *5*, 59–71.

Vodermaier, H.C. (2004). APC/C and SCF: controlling each other and the cell cycle. Current biology: CB *14*, R787–R796.

Zeng, X., Chauhan, C., and Hou, S.X. (2010). Characterization of midgut stem cell- and enteroblast-specific Gal4 lines in Drosophila. Genesis *48*, 607–611.

Zielke, N., Edgar, B.A., and Depamphilis, M.L. (2013). Endoreplication. Cold Spring Harb. Perspect. Biol. *5*, a012948.